DRUG DEVELOPMENT AND INDUSTRIAL PHARMACY, 19(17&18), 2197-2240 (1993)

UNIAXIAL COMPACTION MODELLED USING THE PROPERTIES OF SINGLE CRYSTALS

Wendy. C. Duncan-Hewitt
Faculty of Pharmacy, University of Toronto
19 Russell Street, Toronto, Ontario,
M5S 1A1, Canada.

ABSTRACT

The microindentation technique provides a means of evaluating a number of parameters that characterize the mechanical behavior of single crystals, including plasticity, elasticity, fracture toughness, and the activation volume and activation energy of the associated deformation kinetics. These values have been incorporated into models which predict the pseudostatic compaction and tablet stress relaxation of a number of pharmaceutical materials. Ultimately, the goal is to produce a model to predict dynamic compaction and the strength of the resultant tablet.

INTRODUCTION

The practical goal of the formulator is to produce a tablet which can resist failure prior to administration yet dissolve quickly in the gastrointestinal

tract. While tablets which meet these specifications often can be achieved by the relatively empirical methods of granulation or modification of the method and rate of compaction, these solutions are expensive and they are not always effective. Persistent tablet failure by lamination (splitting horizontally) or by excessive wear during processes such as coating is confounding.

These problems provide the impetus to understand and predict the outcome of the compaction process and to identify and control the factors which influence tablet strength. Also, given the limited amounts of material available from preliminary drug development studies, it would be useful if one could achieve these objectives by testing single particles or crystals.

The attainment of this multi-faceted goal is subject to three prerequisites:

1) The relevant material properties must be specified.

2) A means of quantifying those properties using single crystals must be identified.

3) A link between the behavior of single crystals and parameters that characterize tablet "quality" such as such as density, resistance to lamination, fracture strength, friability, disintegration, and dissolution must be forged.

The modelling process which encompasses these three steps has proven to be a useful tool in the materials sciences but its application in the field of solid pharmaceutics is still in its infancy[1-4].

Empirical evidence has shown that tablet strength is a function both of the intrinsic properties of the material and of extrinsic factors which operate during compaction, handling, and storage. The intrinsic physical properties which have been implicated as important determinants of tablet strength include: 1) plastic

(irreversible) deformability which facilitates the formation of permanent particle-particle contact regions during compaction; 2) elastic (reversible) deformability which can give rise to residual stresses within the compact during the decompression phase of the compaction cycle; 3) fracture toughness, which determines the extent to which the particles or the interparticulate contact regions fracture or crush during compaction; 4) deformation kinetics which determine the relative degree to which elastic, plastic, and brittle behaviors are manifested, and; and 5) surface free energy, which controls the interparticulate bond strength[5-10].

Secondary variables which are believed to affect the densification behaviour of pharmaceutical materials include, particle size, interparticle and die-wall friction, initial packing of the powder in the die, die size, and the range of stresses employed[11,12].

The size of this list alone makes it obvious that a truely comprehensive model of tablet compaction would be extremely complex. Therefore, while the ultimate goal is to be able to predict and control the behavior of a specific formulation in an arbitrary compaction procedure, the achievements to date, while promising, have been much more modest. This paper will review the development, predictions, and limitations of the following preliminary models: 1) the pseudo-static (i.e., slow) compaction of single component tablets consisting of primarily ductile or brittle substances, 2) the in-die stress relaxation of compacts. The requirements for future developments will then be outlined.

Selection Of Relevant Material Properties And Their Quantitation

The primary material properties that would be expected to play a prominent role in one or more of the

simplified situations listed above would be plasticity, elasticity, fracture toughness, and deformation kinetics. Some of the more generally accepted and most easily applied methods of evaluating elasticity (eg. beam bending, dynamic resonance), plasticity (eg., uniaxial tension, bending, torsion), and fracture (eg., 3 or 4 point bending, chevron notch) usually require specimens which are relatively large and which possess a defined geometry. Single, large, relatively flawless organic crystals are difficult to obtain, and the preparation of suitably oriented test specimens is often difficult or impossible. They are inherently brittle, susceptible to thermal shock, and degrade easily under conditions which are usually employed to produce large single crystals or fully dense polycrystalline specimens of other materials. Fortunately, the advent of brittle ceramics that are used in engineering applications has led to the development of microindentation as a materials characterization technique because crack propagation, which renders most other mechanical tests of plasticity almost impossible in these materials, is suppressed in this configuration. For these materials, the microindentation test is the simplest, and often the only mechanical test available. It is a rapid, convenient, and inexpensive method that has been developed to the extent that it can be used to evaluate all the mechanical parameters above using only a few measurements.

Microindentation Test

In the microindentation test, a small, hard (steel or diamond), indenter of a defined geometry is pressed into the surface of a test specimen for a specified length of time. The size of the resulting indentation is a function of the load applied to the indenter so

that very small indentations, on the order of tens of micrometers in diameter, may be produced under well-controlled conditions.

The following variables must be defined in an indentation test: a) specimen size; b) indenter geometry; c) environment (composition, temperature); and d) indentation time. Relatively small loads are required to test most pharmaceuticals since organic crystals are generally quite small (< 2 mm), and soft. Indentations may be measured using optical microscopy. Criteria which maximize precision have been established for each indenter geometry[13,14].

It is important to apply the load slowly and smoothly in the microindentation test, since indentations may be enlarged considerably by any vibrations which occur during the loading procedure. Modern hardness testers are adequate in this regard. However, extraneous vibrations must be avoided.

The specimen must be at least ten times as thick as the indentation is deep, to avoid the need to consider the role of the method of support when calculating the hardness value. For small specimens, this introduces another variable into the analysis, since the relative roles of bulk and surface deformation must then be considered[15].

The use of an indenter which produces indentations whose geometry is independent of the size of the indentation[16] simplifies the analysis, since ideally, the values of the test parameters will then be independent of load. Two types of indenter fit this criterion: the sharp cone, and the pyramid.

The "sharpness" of an indenter plays an important role in governing the mode of deformation of the material during indentation, and also controls the magnitude of the effect of friction. Blunt indenters are

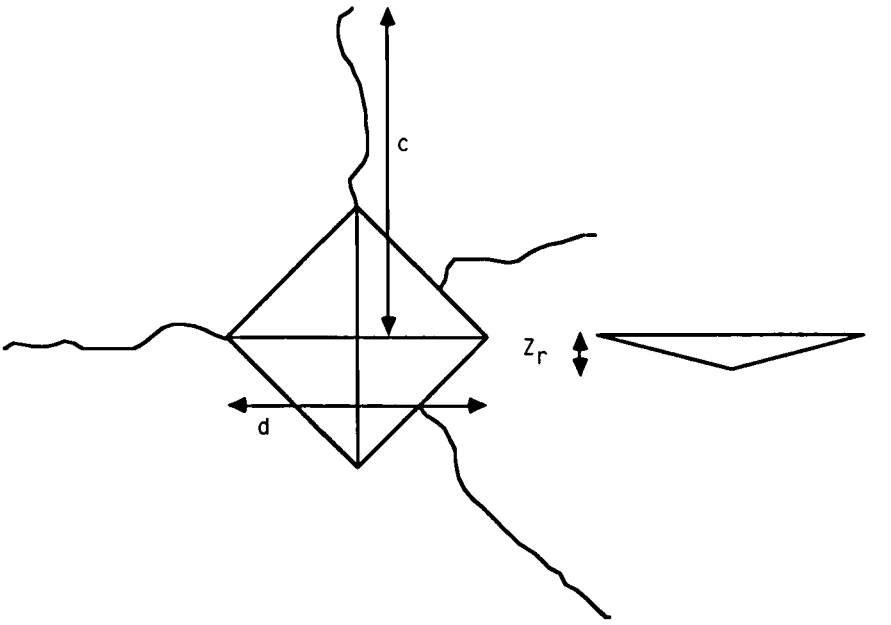

FIGURE 1

A Vickers microindentation showing the critical parameters that are measured to provide estimates of the hardness, elastic modulus, and toughness of the material.

preferable for several reasons: 1) indentation parameters are essentially independent of friction, especially if the indenter is cut from diamond: the coefficient of friction between polished diamond and unlubricated metals ranges from approximately 0.1 to 0.15[17]; 2) the indentations are shallow, therefore the required thickness of the specimen is decreased commensurately; 3) complications due to fracture behaviour occur less frequently; and 4) the two indenters which are employed most frequently are blunt (the 136° Vickers pyramid and the asymmetrical Knoop) and their behaviour is well documented in the literature. Most advanced theoretical studies and routine applications employ these indenter

configurations and instrumentation is readily available.

Hardness and Plastic Flow

The Vickers Hardness (H) is calculated from the mean length of the diagonals of an indentation (Fig. 1) using Eqn. 1, and is equal to the mean stress across the true area of contact.

$$H = 1.854 \cdot P / d^2, \quad MPa \qquad (1)$$

P = load, N
d = Mean indentation diagonal, mm

Hardness and the uniaxial plastic yield stress (the stress at which significant permanent deformation occurs in a specimen that is tested in a uniaxial tension configuration) are correlated by a "constraint factor", which is believed to arise from the interaction between the material which is yielding and the surrounding elastically deforming material. The mechanism of constraint is still not fully understood[18-20]. Empirical correlations between the uniaxial yield stress of metals and their hardness indicate that the constraint factor is constant and approximately equal to 3. For materials which are brittle and elastic the constraint factor varies with the ratio of the yield stress to elastic modulus of the material.

Kinetics of Flow

The fundamental assumptions of the rate theory of plastic deformation[21] are: 1) in the process of flow, energy barriers must be overcome which are similar to those limiting the rate of a chemical reaction; 2) The barrier to deformation is symmetrical at equilibrium

(the probability of deformation is equal in all directions so that no net deformation is observed). When stress is applied the associated elastic work effectively decreases the height of the activation barrier in the forward direction while concurrently increasing the height of the barrier to deformation in the reverse direction; 3) At high levels of stress, the probability of deformation in the forward direction is so much greater than that in the backward direction that, in principle, a single rate constant can be evaluated.

The observed deformation is assumed to be the sum of the contribution of all the mechanisms which are operating concurrently. For the sake of simplicity in the discussion which follows, we shall consider a case in which one mechanism operates; a situation which can be realized experimentally by applying a high level of stress and which probably occurs in practice in the microindentation test and during compaction.

The height of the activation barrier is characterized by the activation free energy:

$$\Delta G^* = k \cdot T^2 \left[\partial \ln (d\gamma/d\tau) / \partial T \right]_{\tau, struct} \qquad (2)$$

ΔG^* = experimental activation energy
k = Boltzman constant (replaced by R for molar quantities)
T = absolute temperature, K
γ = shear strain
τ = shear stress
struct = a measure of the extrinsic factors which limit dislocation mobility such as tangles, impurities

The activation volume, V*, is associated with the size of the deformation region and can be calculated

from the following function of strain rate and stress:

$$V^* = k \cdot T \left[\partial \ln (d\gamma/d\tau) / \partial \tau \right]_{\tau, struct} \quad (3)$$

The activation volume can be interpreted physically. For example, if deformation occurs by molecular diffusion, it will be on the order of the molecular size. On the other hand, if flow is limited by the interaction of many dislocations, the activation volume will consist of the entire region containing the interactions and can be of the order of 1000 times the molecular volume.

The microindentation test has been employed to investigate the deformation kinetics of many metals and ceramics, and also face centered cubic salts such as LiF and NaCl at high levels of stress[22,23]. This fact is particularly fortuitous because the compaction behaviour of these materials has been studied exhaustively in the pharmaceutical literature so that their behaviour can be used as the basis for the development of the deformation kinetic analysis. While it is often the only test available it possesses two major drawbacks that must be considered. Because the deformation field is so complex, consisting approximately of an expanding sphere that presses into the surrounding elastic material, the strain rate is difficult to define, and many different approximations are employed. Verrall et al.[22] used a particularly simple relationship. Noting that the strain, $\varepsilon \sim 0.08$ for a Vickers indentation, they suggested that the strain rate could be approximated by Eqn. 4, the shear strain-rate by Eqn. 5, and the shear stress by Eqn.6.

$$d\varepsilon/dt = 0.08/t \quad (4)$$

$$d\varepsilon_s/dt = 0.08 \cdot \sqrt{3}/t \quad (5)$$

$$\tau = H/(3\sqrt{3}) \quad (6)$$

$d\varepsilon/dt$ = strain rate, s^{-1}
$d\varepsilon_s/dt$ = shear strain rate, s^{-1}
t = time

The latter equation arises from the relationship between the hardness and the shear strength of a material, assuming a constraint factor of 3 and the Von Mises yield criterion[20]. These relationships arise naturally if the change in hardness with time is equivalent to a creep process. The factor of 0.08 is arbitrary. Assuming it is independent of temperature, its magnitude does not affect the results of kinetic analyses.

Elastic Behavior During Indentation Testing

While a number of groups have developed procedures to evaluate elastic moduli from microindentation parameters, the approach developed by Lawn and Howes[24] and subsequently modified by Breval and MacMillan[25], which requires the measurement of the recovered depth of an indentation, is the most versatile. An indentation in a purely ductile material does not recover elastically. Conversely, the depth of an indentation in a highly elastic material will recover substantially. In the purely elastic limit, no permanent indentation remains (Fig. 1). The final relationship (Eqn. 7) fits the experimental data obtained for polycrystalline specimens tested under uniaxial tension. While the validity of the test when performed on single crystals is unknown, it was used in the present research. Validation of the test is currently being undertaken.

$$(2\ Z_r/d)^2 = 0.08168.[1-8.70(H/E)+14.03(H/E)^2] \quad (7)$$

Z_r = recovered depth of indentation (μm)
E = Elastic Modulus (MPa)

Fracture

Many crystalline materials will fracture if they are stressed above a critical level. The value of this stress depends upon the properties of the material, the configuration of the test system, and environmental variables. The science of fracture mechanics was developed to elucidate the fundamental material properties which control fracture behavior, and to discover their relationship with the external variables[26].

The relationship between the stress intensity factor at failure (K_C), often called the fracture toughness, and the fracture stress of a brittle specimen containing a sharp internal crack loaded in simple tension is expressed in Eqn. 8.

$$\sigma_f = (K_C^2 \cdot (1 - \nu^2)/(\pi \ c))^{0.5} \qquad (8)$$

σ_f = fracture stress
ν = Poissons's ratio
K_C = fracture toughness
c = crack length

While the fracture stress varies with the method of loading and the size of cracks within a test specimen, K_C is a constant that ideally, depends only on the mode of crack propagation (eg., tension, shear, torsion). In reality, K_C is also a function of non-equilibrium kinetics, deviations of the crack surface from planarity, plasticity, and other dissipative terms[26]. However, if care is taken during the specification of the conditions under which the test operates, K_C may be considered to be a predictive material property.

Indentation Fracture Mechanics

The field of indentation fracture mechanics has been developed recently[27-31]. While stress intensity factors have been exactly determined for many test configurations, only approximate solutions are available for indentation configurations.

Approximate fracture mechanics solutions are calibrated using values for K_C determined using other methods[32]. The K_C values used in the present research were calculated using the equation developed by Anstis et al.[33] (Eqn. 9) which requires the measurement of radial cracks that form during microindentation (Fig. 1):

$$K_C = 0.016\ (E / H)^{0.5}\ (P/c^{1.5}) \qquad (9)$$

Equation 9 has been calibrated using many single crystal and polycrystalline substances, and has been subsequently employed by others[34]. The fit is excellent for polycrystalline substances, but not as good for monocrystals. However, the fit for single crystals is improved if the calculations are corrected for the angular orientation of the cracks in the crystals[35].

The conditions which obtain during tablet compaction and subsequent processing always entail contact processes. Therefore, the hardness, apparent elastic modulus, and indentation fracture resistance alone provide valuable information, and analytic solutions are not essential.

MODELS OF TABLET COMPACTION[1]

Distinction of "Brittle" and "Ductile" Compaction Behavior

The form of the plot that results when the tablet relative density is plotted vs. the compaction stress

according to the Heckel relationship (Eqn. 10) has been shown to be related to the mechanical properties of the particles.

$$\ln (1/(1-RD)) = K_0 + k_H \cdot PS \qquad (10)$$

RD = relative density
K_0 = constant
k_H = slope of Heckel plot ("inverse mean yield pressure")
PS= compaction stress (punch stress)

A linear Heckel plot is believed to indicate essentially ductile behavior of the particles during compaction, while a curvilinear plot is believed to indicate brittle behavior. Given this fact, and the observation that the compaction of brittle materials is accompanied by considerable particle fracture and asperity crushing whereas ductile particles tend to become rounded and blunted it would seem appropriate to construct two distinct models of compaction to take this mechanistic difference into account.

"Brittleness" factors have been used extensively in the wear literature[36], and appear to be reasonable criteria to differentiate compaction behavior, based on the facts stated above. The simplest brittleness factor is the ratio of fracture toughness to hardness, K_C/H. This "brittleness index", varying from 10 to 50 for brittle materials is of the order of unity for semi-brittle materials such as sodium chloride and two orders of magnitude smaller for metals and polymers divides the materials into two groups (< 5 = ductile; > 5 = brittle) which correctly reflect the two types of Heckel plot and the microscopic behavior of the materials during compaction.

Assumptions Used in Simplified Models of Tablet Compaction

The rate of compaction will be considered to be slow enough that the yield stress is time independent. The effects of the other variables are accounted for as follows:

1) Complications due to elastic deformation are avoided by relating the compaction stress to the density of the compacts once they have been removed from the die, i.e., after elastic recovery has occurred.
2) The effect of particle size is ignored.
3) It is assumed that the particles are all the same size.
4) The effects of die-wall friction are assumed to be the same for all materials. Uniform friction effects can be achieved experimentally by prelubricating the die with magnesium stearate prior to compaction.
5) It is assumed that the density of the tablet was uniform throughout.

Requirements of All Single Particle Models of Tablet Compaction

A model of powder compaction requires:

1) *An expression for the change in the number of particle contacts during densification.*
2) *An expression for the average area per contact as a function of the particle geometry and relative density of the compact.*
3) *An expression for local yielding at the contact.*
4) *An expression for the local stresses at the contact in terms of the far field stresses.*

In general, the simpler these relationships are, the more easily the model is applied. A discussion of the manner in which each requirement is met in the models of tablets compaction follows.

An Expression for the Change in the Number of Contacts Per Particle During Densification

The total force on a particle is directly proportional to the coordination number which gives the average number of nearest neighbors in a packing of equal-sized particles. Since particles rearrange somewhat during compaction, it is probable that the coordination number increases during densification. Several relationships between relative density and coordination number have been described in the literature, ranging from lists of relative densities associated with various perfect packings to descriptions of random packings[37,38]. The relationship described by Arzt[38] was used in the present work.

$$Z = 7.3 + 9.5\ (RD - 0.64), \quad RD < 0.85 \tag{11}$$

$$Z = 7.3 + 2 + 9.5\ (RD - 0.85) + 881\ (RD - 0.85)^3, \quad RD \geq 0.85 \tag{12}$$

Z = coordination number

An Expression for the Average Area Per Contact as a Function of the Particle Geometry and the Average Relative Density of the Compact

I. DUCTILE MATERIALS

It is assumed that the stress response of crystals of fairly uniform shape or habit resembles that of

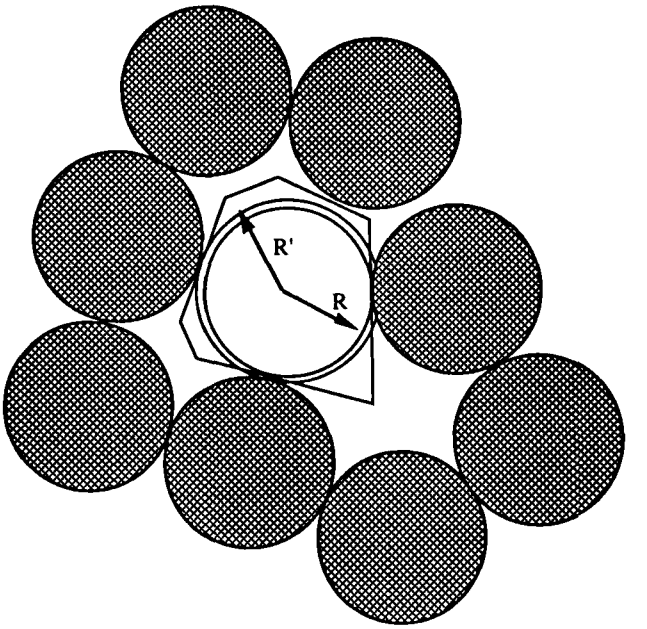

FIGURE 2

The geometry of initial packing and densification in the compaction model for ductile materials.

spheres. While the asperities of the particles are initially angular, small amounts of deformation will tend to round them so it is further assumed that on average, the contacts will deform as sections of spheres.

Arzt[38] developed an elegant model to describe the densification of spherical powders. A spherical particle with an initial radius of unity (R; Fig. 2) is assumed to grow concentrically within its original Voronoi cell[39]. The Voronoi cell is the set of points closer to a particle's centre than to any other particles centres. When the particle contacts and overlaps a face of the cell (R', Fig. 2), the volume of the material removed by the contact is assumed to be distributed evenly across the remaining free surface of the par-

ticle increasing the apparent particle radius further (R''). The following relationships which provide an expression for the average contact area in terms of the relative density were derived (Equations 13):

$$R' = (RD / RD_i)^{0.33} \quad (13a)$$

$$V_{ex} = S_f \cdot (R''^3 - R'^3) / (R'^2 \cdot 3) \quad (13b)$$

$$R^* = R' - 1 \quad (13c)$$

$$V_{ex} = R^{*2} (\pi Z_i / 3) (2 R' + 1) + R^{*3} (C \pi / 12) (3 \cdot R' + 1) \quad (13d)$$

$$S_f = (4 \cdot \pi \cdot R'^2) - (2 \cdot Z_i \cdot \pi \cdot R' \cdot R^*) - (C \cdot \pi \cdot R' \cdot R^{*2}) \quad (13e)$$

$$A = [\pi / (3 Z R'^2)] \cdot [3 Z_i (R''^2 - 1) + C + R''^2 C (2 R'' - 3)] \quad (13f)$$

RD = present relative density
RD_i = initial relative density
S_f = free surface remaining on sphere
R'' = present radius of sphere with deposited material
R' = enlarged radius of sphere before material deposition
V_{ex} = volume of material cut off by face of Voronoi cell
Z_i = initial coordination number
Z = present coordination number
C = 15.5, a constant
A = average contact area

II. ANGULAR PARTICLES OF BRITTLE MATERIALS

Most models of densification assume that the particles are spherical. Crystals of many brittle drugs and excipients are acicular, platy, cubic, etc. and remain that way during compaction. A spherical contact model is not adequate for these materials. For model-

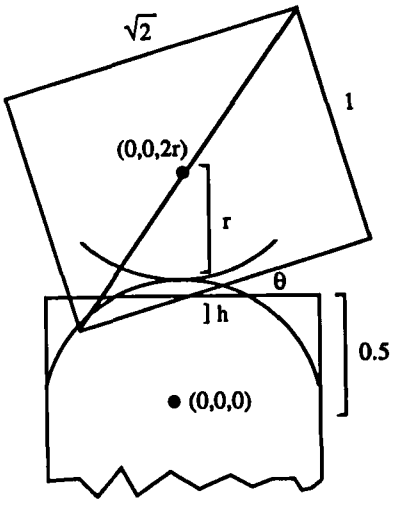

FIGURE 3

The geometry of particle packing and densification in the compaction model for brittle materials.

ling purposes it is assumed that the particles are cubic, and contact each other at cube corners only.

The initial packing of the powder will be a function of the average relative misorientation of the particles. As densification proceeds the area of contact between a surface and a corner of a rectangular parallelepiped, the latter being crushed by contact with the surface, is controlled by their relative orientation, which may be defined by rotations around 2 axes which pass through the centre of the particle. Fig. 3 illustrates one such orientation, a tilt of θ degrees around the diagonal of a cube face. For this case the height of the crushed asperity (h) is related to the area of contact (A) by the expression:

$$A = h^2 \cdot (\tan(\theta) + \tan(90-\theta)) / \sin(\theta) \qquad (14)$$

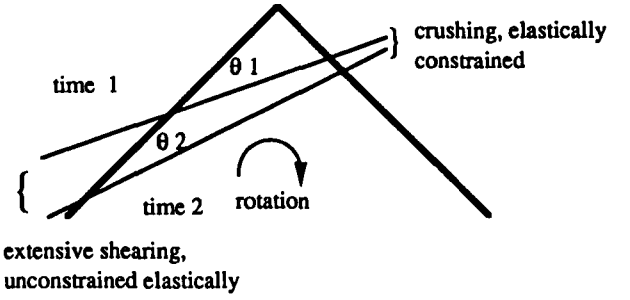

FIGURE 4

The effect of particle rotation on the deformation behavior at the interparticulate contact region.

Since rotation around the diagonal simplifies subsequent calculations and decreases the number of assumptions required in modelling, this geometry will be used whenever angular asperities are considered below. The error introduced by this assumption is at most 5%.

When angular crystals contact each other, rotation moments will invariably develop. Therefore, unless the crystals are restricted by mechanical interlocking or extremely high frictional forces, they should rotate relative to one another during compaction. The present model assumes that crushing and the rate of particle rotation are governed by the constraints which inhibit the removal of the fragments from the interface. As the particles rotate relative to each other, the angle θ (defined in Fig. 3) decreases, the asperity crushes further, and the particles can move closer to each other as fragments are displaced (Fig. 4). The fragments which are near the side of the asperity which is adjacent to θ in Fig. 4 are subjected to intense shearing. Flow occurs laterally, and is therefore relatively unconstrained. At the opposite edge of the asperity, normal stresses inhibit the removal of fragments, there-

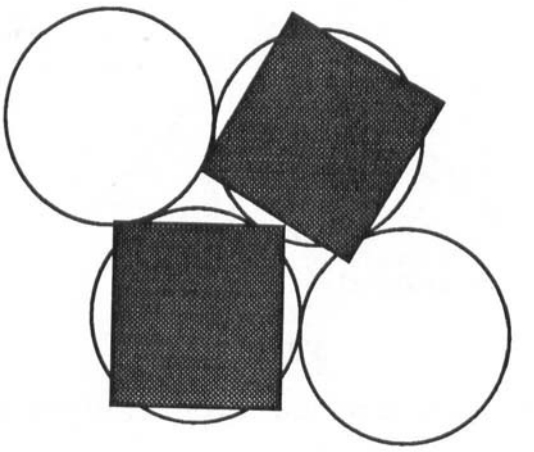

FIGURE 5

The initial packing model for the densification of brittle materials. Each cubic particle is located at the centre of a sphere of equal volume. The spheres are "randomly close packed".

fore the configuration at this location resembles indentation. The simplest approximation of the relative rates of removal of fragments from each edge of the asperity should then be the ratio of the hardness to shear strength of the material.

For brittle organic materials, the hardness to shear strength ratios can be estimated from the indentation constraint factor using the expression given by Marsh[19]:

$$H / Y = 0.28 + 0.6 \cdot \ln(0.7 \cdot E / Y) \qquad (15)$$

Y = uniaxial yield stress, MPa

For the three organic crystals studied to date, the expression gives values of H/Y = 2.95 (sucrose); 2.71 (adipic acid); 2.39 (acetaminophen).

The next step is to relate the interparticulate contact area with the relative density of the compact. A cubic particle of unit volume is assumed to be oriented randomly within a spherical cell (Fig. 5), many of the latter being packed randomly (RD_i = 0.601[40]). These may be visualized as the spheres in the Arzt model (see Fig. 2 above) arranged within their Voronoi cells. The sphere is assumed to possess a volume of unity when the relative density of the entire assembly is equal to 0.601. The spherical cells provide a geometric reference to describe the densification in terms of particle rotation and asperity crushing.

The particle is oriented within the cell so that it touches the others surrounding it. The actual number of contacts is assumed to be governed by the coordination number for the spherical "cells" as described above in Eqns. 11 and 12.

During densification, the cube remains the same size but the spherical reference cell contracts. As the reference sphere contracts, the cubic particle must either rotate or be crushed at its asperities to accomodate the decrease in volume. The debris resulting from crushing is displaced to the void spaces and is assumed to bear no load. An increase in coordination number with relative density occurs as the asperities of the angular particles impinge upon particles within other cells.

The area of contact between two particles and the radius of the cells is related through h, the present height of the crushed asperity, and Á, the present angle between the two particles (Eqns. 15a and b).

$$y / (\sqrt{3}/2) = \sin(35.2644 + \theta) \quad (15a)$$

$$(y - h - 0.5) / 2 + 0.5 = r \quad (15b)$$

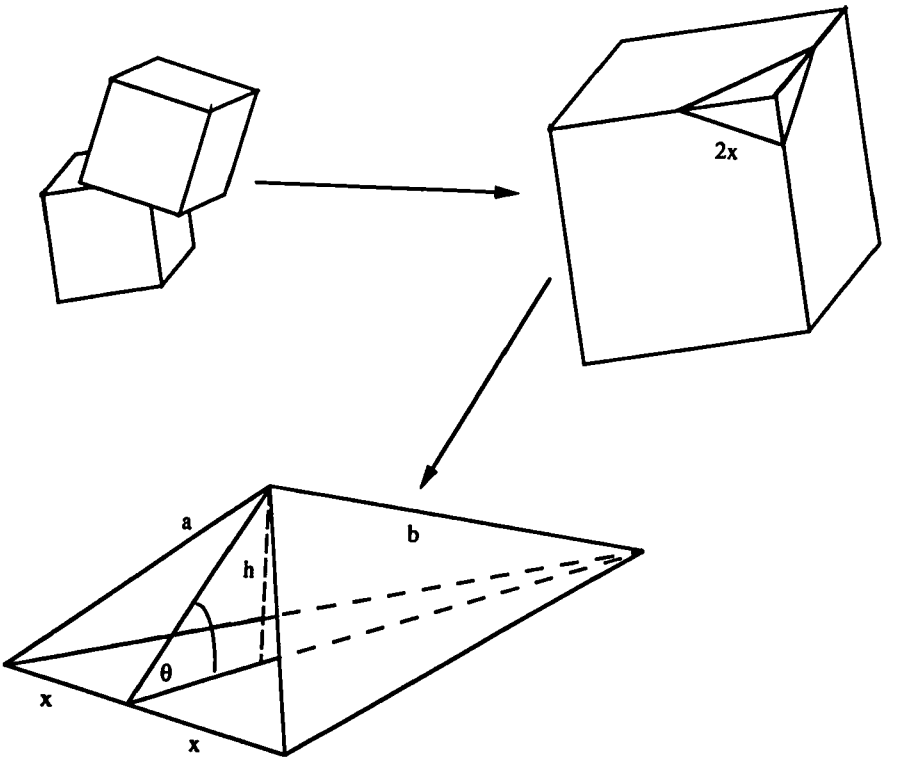

FIGURE 6

The model geometry of the crushed asperity of a brittle particle during densification.

Figure 6 illustrates the geometry of the contact and the definitions of the quantities y, h, and r.

The relative density at any given instant may be found directly from r, the radius of the reference sphere by noting that the true volume of the material associated with one reference sphere is always unity (i.e., V* = 1), and that the ratio of the volume of the reference sphere and the total volume is a constant (Eqns. 15c and d).

$$RD = V^* / V_{total} = 0.601 / V_r \qquad (15c)$$

$$V_r = 4\pi/3 \cdot r_r^3 \qquad (15d)$$

V^* = volume of crystal within reference sphere (= unity)
V_r = volume of reference sphere
r_r = radius of reference sphere

Densification is then modelled as follows:

1) The initial values of "a" and "b" are found from the initial value of h. The latter is found from the initial compaction stress and relative density values, the boundary conditions of the model.
2) For a series of increasing "a" values, each corresponding "b" value is calculated from the relative orientation of the cells at (RD_i, F_i) and a linear regression slope which is equal to the constraint factor of the material (16a). This is equivalent to assuming that the "relatively unconstrained side" of the asperity grows faster than the "relatively constrained side" of the asperity by a factor which is equal to the ratio of the hardness and the shear strength of the material in question.
3) The corresponding angle of orientation is then calculated using equation 16b, and each increasing crushed asperity height (h), using 16c.

$$b - b_i = \sqrt{3}\ CF\ (a - a_i) \qquad (16a)$$
$$\theta = \tan^{-1}(a / b) \qquad (16b)$$
$$h = a \sin(90 - \theta) \qquad (16c)$$

An Expression For Local Yielding At The Contact

I. ISOSTATIC COMPRESSION

Under hydrostatic loading, two contacting particles experience large normal forces and little shear at

their interface. This configuration resembles that which obtains during the mutual indentation of two sharp bodies. Yielding occurs at approximately 3 times the yield stress of the material. This value equals the hardness of the material determined by microindentation techniques, and the most appropriate relationship for local yielding in this loading configuration is represented by Eqn. 17.

$$\sigma_{ct} = H = F_c/A \quad (17)$$

σ_{ct} = contact stress
F_c = contact force
A = area of contact

II. UNIAXIAL COMPRESSION

Uniaxial loading of a mass of particles in a die superimposes shear stresses on the hydrostatic stresses. The extensive shearing that occurs during uniaxial compression increases the probability that the particles will rearrange during compaction. Schwartz and Holland[41] found that the slope of the Heckel plot for iron (1/mean yield value) derived from isostatic compaction was $4.9 \cdot 10^{-8}$ MPa^{-1}, while those quoted by Heckel for iron powders undergoing uniaxial compaction, ranged from $1.1 \cdot 10^{-7}$ to $1.4 \cdot 10^{-7}$ MPa^{-1}. While they attributed this effect to the presence of fines, it is more likely that shear, while not *causing* densification, facilitates it[42].

III. DUCTILE MATERIALS

While the contact area in the absence of shear stresses will be governed by the hardness, any tangential movement will enlarge the area of contact if the material is ductile[43]. It is certain that the average

contact area will be larger than that which may be characterized by the hardness value, and smaller than that characterized by the shear strength. Therefore, some average proportionality between the shear strength and the contact stress must characterize uniaxial compression at various ratios of punch to die-wall stress.

The following approach was used to calculate the proportionality between the mean contact stress in the die and the shear strength of the material.

1) It was assumed that the proportionality was equal to 1 for orientations where the interparticulate shear stress was greater that the normal contact stress.
2) It was assumed that the proportionality was equal to 5.2 if shear stress was equal to zero.
3) It was assumed that the proportionality varied linearly from 1 to 5.2 between the directions at which the two limiting conditions obtain.

For a punch to die-wall stress ratio of 2.5:1 (the average ratio observed during uniaxial compaction of pharmaceutical materials), the average of these values was 3.4. It was assumed that this provides a reasonable approximation of the true value given the number of assumptions required to calculate it.

Therefore, for ductile materials in uniaxial compression, the contact stress will be assumed to be calculated using Eqn. 18.

$$\sigma_C = H / 3.4 = F_C / A \qquad (18)$$

The hypothesis that shear facilitates consolidation provides a means of explaining the effect of lubricants and glidants on the densification process. These materials facilitate densification, but weaken the resultant compact. Since very thin layers of lubricants are present on the surfaces of the crystals, they

would play a minor role if only normal stresses caused densification.

Brittle Materials

As two brittle particles are pressed together, their asperities yield by crushing rather than by flow. Therefore the crushing strength of an asperity must be determined. The origin of the compressive strength of materials has been explained by several theories[44,45] which predict that the compressive strength should be several times greater than the tensile strength. Rice[46] asserts that microplasticity may give rise to compressive failure since the yield stress is the upper limit of compressive strength of many materials.

This theory may be used to develop a model of densification due to crushing, since it provides a yield criterion. Since plastic yielding controls fracture, and since the constraint of the contact geometry increases the apparent yield value by a factor of ~ 3, the hardness should approximate the crushing strength and therefore the proportionality between the normal load and the contact area, as obtains during isostatic compaction (see above). Microplasticity appears to play a role in the fracture which is observed during indentation[33], and therefore Rice's theory appears to be well-suited to the mechanical behavior of brittle materials. Eqn. 17 will be used to describe the contact stress for brittle materials.

An Expression for the Local Stresses at the Contacts in Terms of the Far Field Stresses

I. RELATIONSHIP BETWEEN UNIAXIAL COMPACTION STRESS AND THE MEAN STRESS WHICH CAUSES Ddensification

Die compaction differs from isostatic pressing since the load is applied from one direction only. It

is assumed that densification is caused by the hydrostatic component of the stress within the die, which is smaller than the punch stress, while the shear component of the stress causes only changes in shape[47].

The hydrostatic component may be calculated as the mean of the principal stresses within the die. This calculation is not trivial, since the effects of friction and the discontinuous nature of the powder compact will cause rotation of the direction of the principal stresses with increasing depth and radius within the compact, and in fact, will probably change from particle to particle. Therefore, to simplify the problem, it will be assumed that the first principal direction is parallel to the axis of the die; the others are perpendicular to this, but otherwise are arbitrarily directed ($\sigma_y = \sigma_z$). The ratio of the die-wall stress (σ_y) to the punch stress (σ_x) has been measured for sodium chloride[48,49] and sucrose[49,50], and appears to be essentially constant for σ_x values between 0 and 197 MPa. The mean stress (MS), assumed to be equal to the hydrostatic component of stress will be calculated as the mean of these assumed principal stresses (Eqn. 19).

$$MS = \bar{\sigma} = (\sigma_x + \sigma_y + \sigma_z)/3 \quad (19)$$

MS = mean stress, assumed to be equal to the hydrostatic component of stress
σ_x = punch stress
σ_y, σ_z = die wall stresses

II. RELATIONSHIP BETWEEN THE MEAN COMPACTION STRESS AND THE AVERAGE FORCE AT ONE CONTACT

Since the hydrostatic stress, approximated by the mean stress in the die, gives rise to densification, it is assumed that the mean compaction stress is distrib-

uted over the surface of a sphere enclosing the particle whose deformation is being considered. The average relative density of the contents of the sphere is equal to the present relative density of the compact and the average force on each particle contact region is determined by the coordination number at any given time. The volume of the sphere is calculated as follows.

1) *Ductile Materials:* It is assumed that the size of the Voronoi cell (or equivalently, the reference sphere over which the external stress is distributed) is constant, while the particle within grows. Then the surface area of the reference sphere also remains constant and may be calculated from the initial relative density using Eqn. 20.

$$RD_i = V_p / V_r \quad (20a)$$

$$V_r = 4 \cdot \pi \cdot r_r^3 / 3 \quad (20b)$$

$$SA_d = 4 \cdot \pi \cdot r_r^2 \quad (20c)$$

V_p = particle volume
V_r = volume of reference cell
r_r = radius of reference cell
SA_d = surface area of the external reference, ductile material

2) *Brittle Materials:* The volume of the particle is assumed to be equal to unity, while the volume of the external reference sphere is assumed to decrease. The geometric reference sphere must contain the particle and sufficient void space so that the average relative density of the contents is equal to the present relative density of the compact. The volume of the sphere over which the mean compaction stress is distributed is then equal to the inverse of the relative

density. The surface area of this sphere is found using Eqn. 21.

$$RD = V^*/ V_r = V_r^{-1} \quad (21a)$$

$$r_r = (0.75\ \pi\ RD)^{0.33} \quad (21b)$$

$$SA_b = 4\ \pi\ r_r^2 \quad (21c)$$

V^* = volume of crystal within cell ($V^* = 1$)
SA_b = surface area of reference sphere, brittle materials

For both brittle and ductile materials, the local contact stress is then related to the far-field stresses using Eqn. 22.

$$MS = Z\ F_c / SA \quad (22a)$$

$$F_c = \sigma_c\ A \quad (22b)$$

Z = coordination number
F_c = force on one contact
σ_c = contact stress
A = area of contact

Application of the Models to Predict the Compaction of Some Pharmaceutical Materials

I. DUCTILE MATERIALS

The model is applied as follows:

1) the initial relative density is that of the powder before consolidation begins;
2) a set of increasing relative densities is prescribed;
3) the coordination number for each relative density is calculated using Eqns. 11 and 12;

4) the contact area per asperity is calculated as a function of the relative density using Eqns. 13;
5) the total force per particle is calculated using Eqn. 18;
6) the hydrostatic or mean stress is calculated using Eqns. 20;
7) the punch stress is calculated from Eqn. 19.

In summary, this procedure calculates the punch stress at each prescribed relative density during uniaxial compaction from the mechanical properties of the ductile crystals being considered. The densification of sodium chloride was predicted using the average ratio of punch stress to die wall stress found in the literature, 0.4[48,49,51], and the hardness which was determined experimentally by microindentation (213 MPa). The predicted and experimental curves coincide within the range of the experimental variability associated with the hardness values and the compaction data (Fig. 7). It is obvious that accuracy of the hardness is crucial to the agreement between theory and experiment.

II. BRITTLE MATERIALS

Construction of the densification curve requires knowledge of the initial stress applied to permit accurate measurement of the initial relative density. Point contacts, which in theory might be correlated with the initial powder packing, cannot occur since the weight of the particles alone will cause some crushing.

The following sequence is used to calculate the densification curves.

1) The initial mean stress is calculated from the punch and die-wall stresses using Eqn. 19.
2) The initial force per contact is calculated by multiplying the mean stress by the initial surface

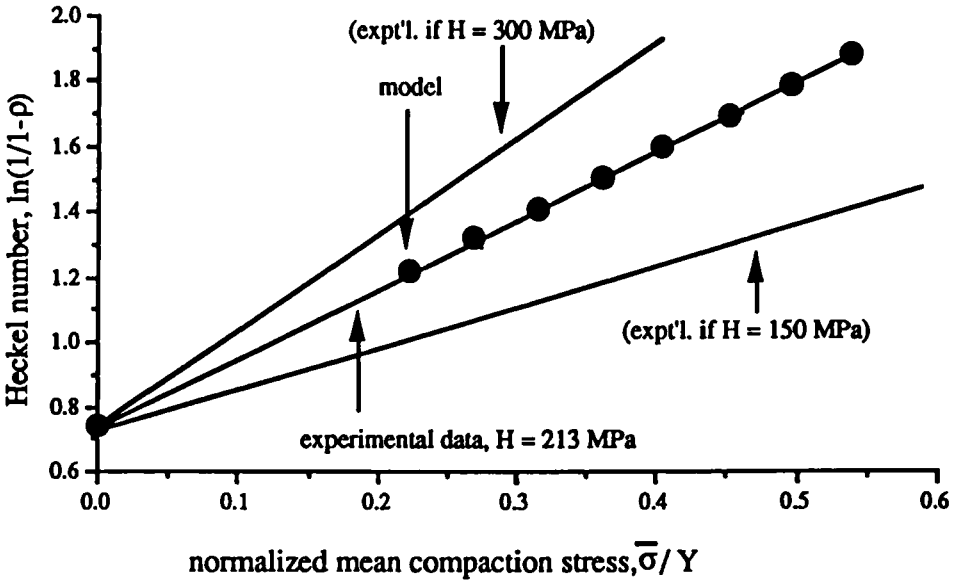

FIGURE 7

The Heckel plot for sodium chloride. The model fits the experimental data if the crystal hardness is 213 MPa, the value measured experimentally. The lower and upper curves show the model predictions for the lower and upper hardness limits for sodium chloride that have been reported in the literature.

area of a sphere of the same relative density as the compact (Eqn. 21) and dividing by the coordination number at that relative density (Eqns. 11 and 12).

3) The second spherical reference is selected so that it possesses the same volume as the particle ($V^* = 1$) when the relative density of the powder is 0.601 (i.e. "loose random-packed").

The next step involves an iterative process. A radius R_o which is greater than the radius of the reference sphere is arbitrarily selected to represent the size of the reference cell when the cubes just contact each other. The initial angle θ is

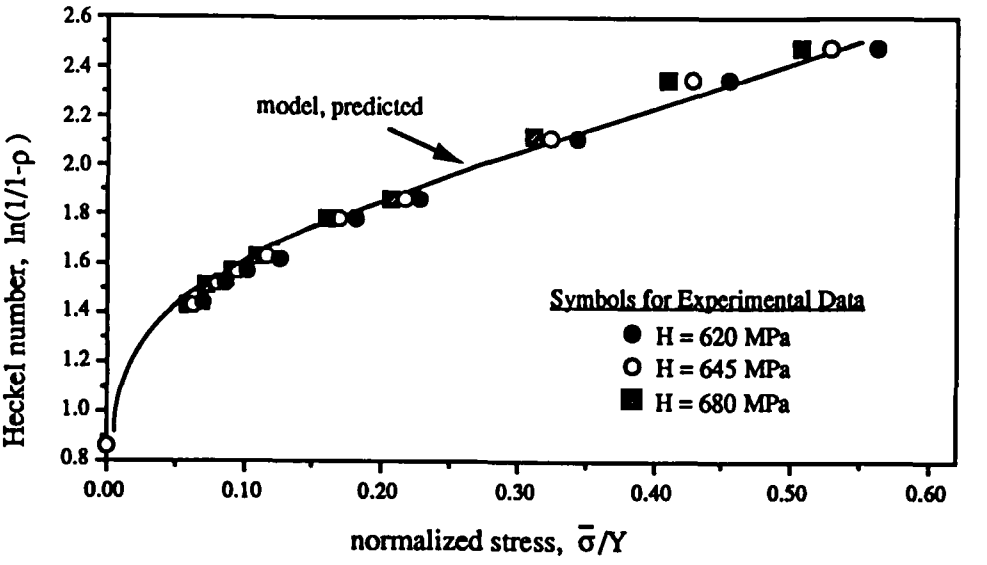

FIGURE 8

The Heckel plot for sucrose. The curve indicates the model prediction.

found from the length of the cube diagonal ($\sqrt{3}$) and the fact that the reference spheres just touch (i.e., distance from centre to centre is 2R). Twice the difference between the arbitrary radius, R_o, and that of the reference sphere gives h at the beginning of the experiment. The contact force corresponding to this value of h may be calculated from Eqns. 14 and 17 and the hardness of the material. This contact force is compared to that calculated in step 2. The length R_o is varied until the contact forces in step 3 and step 2 are equal. At this point, the initial values of θ and h are set.

4) The initial values of a and b (Eqn. 16) are found from h in step 3.

5) The value a is increased in a stepwise manner; b is calculated from Eqn. 16a and h can then be found from 16b and 16c.

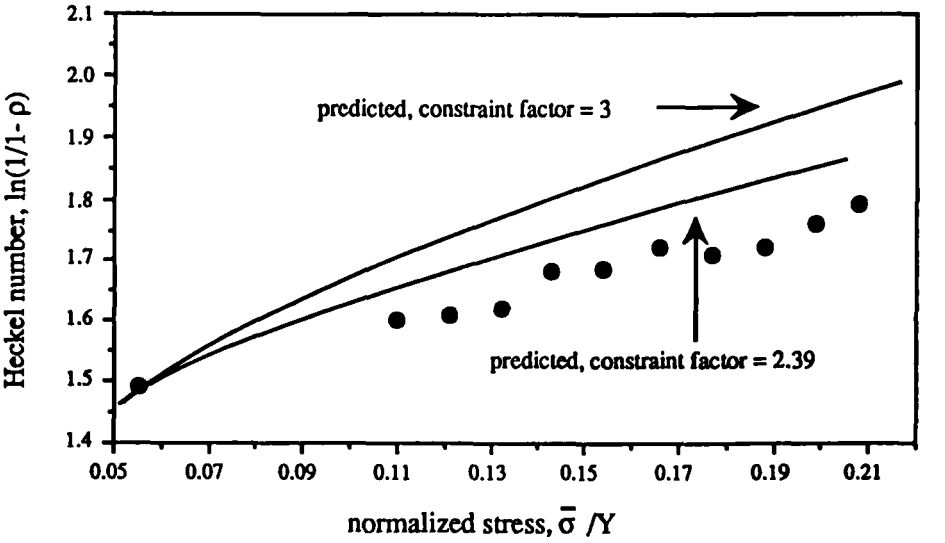

FIGURE 9

The Heckel plot for acetaminophen. The curves indicate the model prediction for constraint factors of 2.39 (that measured experimentally) and 3 (that of a perfectly plastic material), respectively.

6) The new contact area, and from this value, the contact stress, are calculated using Eqn. 14.
7) The relative density is calculated using Eqn. 15.
8) The mean stress may then be calculated from the present coordination number and the surface area of a sphere, the contents of which possess the present relative density (i.e., in effect steps 1 and 2 are carried out in reverse).

While the densification of sucrose (Fig. 8) is predicted by the model to within experimental error (the upper and lower hardness values seen in the figure), the compaction behavior of acetaminophen (Fig. 9) is not. The lack of fit for the latter material may arise from elastic effects: laminations which were observed in this study but which did not cause the tablet to fail completely could give rise to measured relative

densities which are smaller than the true relative densities by a factor related to the volume of the crack.

Fig. 9 also shows the effect of varying the magnitude of the constraint factor. The upper predicted curve was calculated using a constraint factor of 3 (i.e., the constraint associated with rigid/plastic behavior observed with "ductile" materials). The lower curve, which appears to predict the experimental behavior better, was predicted using a constraint factor which was calculated using the Marsh expression (Eqn.15) and the ratio of H/E determined experimentally.

Model Of Tablet Stress Relaxation

Attempts to use linear viscoelastic theory to predict and explain tableting have had very limited success. A combination of a linear spring and dashpot predicts a linear semi-logarithmic relationship between stress and time but does not fit the experimental data for the stress relaxation of sodium chloride[52]. An adequate fit of the same data could be achieved if a large number of mechanical elements are introduced. However, although the resulting "relaxation spectrum" *fits* the data, the associated parameters cannot be interpreted in terms of physically meaningful material parameters. Furthermore the accuracy of experimental data limits the number of constants which can be determined with any confidence. Finally, the slope of the stress relaxation plots change with porosity. Although this is far from surprising, it means that the stress relaxation slopes cannot be interpreted because the role of porosity has not been considered explicitly.

Using compacts of sodium chloride as a model, Papadimitropoulos and Duncan-Hewitt[53] showed that the ki-

netics of in-die stress relaxation can be interpreted using the theory of deformation kinetics[21] through two intermediate models, one which gives the average cross-sectional contact stress in terms of the punch stress (compact model), and the other, which permits the activation parameters to be determined from the punch stress relaxation kinetics (nonlinear three-element model).

Assumptions

It is assumed that stress relaxation experiments are carried out at intermediate levels of stress. Under these conditions, much of the particle deformation is concentrated in the interparticle contact regions which in many cases can be assumed to be oriented randomly within the tablet matrix. Then one need consider only the viscoelastic response at the interparticulate contacts. It is further assumed that the levels of stress and strain-rate are high in these zones so that one mechanism of deformation controls the kinetics as discussed above. Therefore, it is necessary to calculate the parameters of one deformation barrier only.

Finally, it is assumed that the yield behavior, or hardness, is independent of the strain history.

Compact Model

Tablet stress relaxation (measured as a function of the change in force on a punch possessing a defined surface area) can be linked with the deformation kinetics of singles particles by noting the fact that the microindentation test resembles the interparticulate contact configuration. The specific task is to calculate the interparticulate contact area as a function of the true contact area between the compact and the punch. The model must also account for the fact that

the rate of stress relaxation is a function of porosity. The following fulfills these criteria.

In a microindentation test a defined load is lowered onto the surface of a test specimen and is allowed to remain there for 10 seconds after the load is applied fully. The load and final contact area are measured and together these measurements permit the hardness to be calculated. In stress relaxation a defined initial load is applied also, however the force is measured not only at the 10 second point, but continually for an extended period. But the significance of the 10 second point is not lost. In fact, we know that the true punch contact stress must equal the hardness then. Given the hardness and the punch force, one can calculate the true punch/compact contact area immediately. In other words, the contact stress at the ten second point will equal the hardness, independent of the maximum load applied to the punch. What differs at this time is the true contact area between the punch and the particles, which increases with increasing load.

To permit deformation kinetic analysis of the entire stress relaxation curve, it is assumed that the contact area generated during compaction does not change during stress relaxation. Instead, the decrease in stress occurs due to the interchange of elastic and plastic strain within a large, hemispherical deformation region underlying the contact zone. Both experimental and theoretical studies have shown that much of the deformation occurring during the indentation of a viscoelastic material does indeed occur within the crystal bulk[17]. The assumption is further justified by the fact that the compaction process imposes strain and not stress on the compact so that once the movement of the punches has ceased there is decreased impetus for

the particles to continue to approach one another which is the driving force for contact area enlargement.

At intermediate levels of stress, very little total particle deformation occurs in the Hertzian sense (Hertzian deformation can be visualized by imagining the response of a rubber ball when it is pressed between two flat surfaces). At higher levels of stress, these conditions no longer apply and it is necessary to consider elastic deformation of the entire particle also. Contact area enlargement that could arise as a result of the relaxation of the entire particle would cause the apparent stress to fall more quickly than predicted by the current model.

If one makes these assumptions, then the punch force may be normalized by the true contact area at 10 seconds and the resultant "true" stress relaxation curve should be independent of the maximum force applied to the punch. All relaxation curves should then become superimposed. However, if strain hardening occurs, then the contact stress/area relationship would no longer be constant and should result in non-overlap of the normalized relaxation curves.

Non-Linear 3-Element Model

Deformation kinetic analysis permits the evalution of the activation volume and free energy of one barrier to deformation from the strain rate observed in a test specimen if conditions assure that the rate is controlled by that one barrier. When deformation kinetics is used to evaluate *stress relaxation* one is required to couple activation theory with a model which relates stress and strain rate because the strain rate is not measured directly in this type of experiment. As has been shown to be true for many materials, a non-linear 3-element model provides the necessary link for many materials[21].

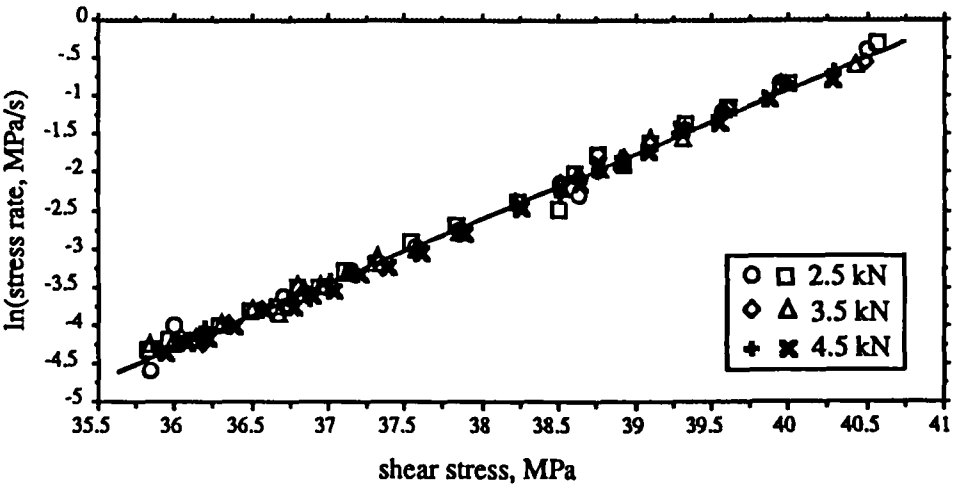

FIGURE 10

Plots of the natural logarithm of the rate of shear stress relaxation versus the shear stress for sodium chloride compacted at a maximum load of 2.5, 3.5, and 4.5 kN. The tablet model causes the curves to be superimposed. The slope of the line is used to calculate the activation volume.

Materials, the behavior of which is adequately described by this model, exhibit a linear relationship between stress and log time in a stress relaxation experiment:

$$\dot{\tau} = - E \dot{\gamma} = - E A \exp[V^*/kT] \quad (23)$$

$\dot{\tau}$ = shear stress rate
$\dot{\gamma}$ = shear strain rate
E = combined elastic modulus of the three element model
V^* = experimental activation volume
A = temperature dependent preactivation factor

Application of the Models to Evaluate Activation Parameters from Stress Relaxation Experiments

Papdimitropoulos and Duncan-Hewitt[53] monitored the stress relaxation of sodium chloride compacts which were formed using maximum loads ranging from 3 to 5 kN for two minutes at 298K. When the relaxation curves were normalized and plotted, they were found to be straight and were superimposed (Fig. 10[53]). This observation supports the hypothesis that the deformation behavior is adequately described by the nonlinear three element model, that the interparticulate contact regions do not enlarge during relaxation, and that strain hardening is not significant.

The activation volume (54 b^3, where b is the Burgers Vector and equals 3.99×10^{-10}m for NaCl) was calculated from a plot of ln (shear stress rate) vs shear stress using Eqn. 23 and is of the order of magnitude indicative of a Peierls-Nabarro mechanism[21], literature values for which range from 3.3 to 100 b^3 for this material[54]. The variability in the literature values probably arises from the extreme sensitivity of the deformation of this material to impurities[55].

The activation free energy was calculated using a plot of ln (stress rate at 201 MPa.s^{-1}) versus 1/K and Eqn. 2 from the results of relaxation tests performed between 25°C to 100°C. The resulting value of 2.0×10^{-19}J) was statistically indistinguishable from the theoretical activation energy which ranges from 1.2 to 3.6 x 10^{-19} J.

GENERAL CONCLUSIONS

The preceding discussion has provided a rationale for modelling the behavior of compacts using the prop-

erties of single crystals, outlined the development of three particular models, and demonstrated the relative success of the approach. This success provides the impetus for attempting to predict more complex situations. Consider the problem of capping, for example.

The compacts of some materials are observed to split horizontally as they are being ejected from the die. The problem is observed more frequently as the rate of compaction is increased and probably arises from a combintation of the effects of excessive residual elastic strain and inadequate interparticulate bonding. A single particle model which might be predictive would possess, in addition to the requirements listed above, the following components: 1) a link between deformation kinetic theory and the viscoelastic deformation of the particle itself as well as the contact regions; 2) a mechanical model of the mechanism of failure, and 3) a relationship between the failure strength of the contact regions and the compact failure strength. Once again, it is probable that brittle and ductile materials will behave differently. Investigations in this area are currently underway.

REFERENCES

1. Duncan-Hewitt, W.C., Ph.D. Thesis, University of Toronto, 1988.
2. Duncan-Hewitt, W.C., and Weatherly, G.C., J. Pharm. Sci. 1990, 79, 147.
3. Duncan-Hewitt, W.C., and Weatherly, G.C., J. Pharm. Sci. 1990, 79, 273.
4. Duncan-Hewitt, W.C., and Weatherly, G.C., J. Mater. Sci. Lett. 1989, 8, 1350.
5. York, P., J. Pharm.Pharmacol., 31 (1979) 244

6. Fell, J.T., and Newton, J.M., J. Pharm. Sci.,1971, 60, 1428.
7. Rue, P.J. and Rees, J.E., J. Pharm. Pharmacol., 30 (1978) 642.
8. Huffine, C.L., and Bonilla, A.I. Ch. E. J., 8 (1962) 490.
9. Hiestand E.N., and Smith, Powder. Technol., 38 (1984) 145.
10. Rippie, E.G., and Danielson, D.W., J. Pharm. Sci., 70 (1981) 476.
11. Fell, J.T., and Newton, J.M., J. Pharm. Sci., 60 (1971) 1866.
12. Lammens, R.F., Liem, T.B., Polderman, J., and de Blaey, C.J., Powder Technol., 26(1980) 169.
13. O,Neill,H., Hardness Measurement of metals and alloys, 2nd edn., Chapman and Hall, London, 1967.
14. Thibault, N. and Nyquist, H.L., Trans. A.S.M., 38 (1947) 271.
15. Westwood, A.R.C. and MacMillan, N.H., in the Science of Hardness Testing and its Research Applications, J.H. Westbrook and H. Conrad eds., ASM, Metals Parks, OH, 1973, p.377.
16. Hill, R. The Mathematical Theory of Plasticity, Clarendon Press, Oxford, 1950.
17. Shaw, M.C., in the Science of Hardness Testing and its Research Applications, J.H. Westbrook and H. Conrad eds., ASM, Metals Parks, OH, 1973, p.1.
18. Tabor, D., The Hardness of Metals, Clarendon Press, Oxford,1951.
19. Marsh, D.M., Proc. Roy. Soc.A., 279(1964) 420.
20. McClintock, F.A., and Argon, A.S., Mechanical Behaviour of Materials, Addison-Wesley Pub. Co., Reading, MA., 1965, 276.
21. Krausz, A.S., and Eyring, H., Deformation Kinetics, J. Wiley and Sons, New York, 1975.

22. Verrall, R.A., Fields, R.J, and Ashby, M.F., J. Am. Cer. Soc., 60 (1977) 211.
23. Goodman, D.J., Frost, H.J. and Ashby, M.F., Phil. Mag., A43 (1981) 655.
24. Lawn, B.R., and Howes, V.R., J. Mat. Sci., 16 (1981) 2745.
25. Breval, E. and MacMillan, N. H., J. Mat. Sci. Letters, 4 (1985) 741.
26. Lawn B.R. and Wilshaw, T.R., The Fracture of Brittle Solids, Cambridge University Press, London, 1975.
27. Lawn, B.R. and Swain, M.V., J. Mater. Sci., 10 (1975) 113.
28. Lawn B.R., and Wilshaw, T.R., J. Mater. Sci., 10 (1975), 179.
29. Laugier, M.T., J. Mat. Sci Letters, 6 (1987) 355.
30. Liaw, B.M., Kobayashi, A.S., Emery, A.F., in Deformation of Ceramic Materials II, Tressler, R.E., and Bradt, R.C., eds., Plenum Press, N.Y., 1984, 709.
31. Marshall, D.B., Lawn, B.R., and Evans, A.G., J. Am. Cer. Soc., 65 (1982) 561.
32. Almond, E.A., Roebuck, B., and Gee, M.G., in Science of Hard Materials, E.A. Almond, C.A. Brookes, R Warren eds., Inst. of Physics conference series number 75, Adam Hilger Ltd., Boston, 1986, 155.
33. Anstis, G.R., Chantikul, P., Lawn, B.R., and Marshall, D.B., J. Am. Cer. Soc., 64 (1981) 533.
34. Pisarenko, G.G., in Advances in Fracture Research (Fracture 84), Vol. 4, S.R. Valluri, D.M.R., Taplin, P. Rama Rao, J.F. Knott and R. Dubey eds., Pergamon Press, Oxford, England, 1984, 2711.
35. Evans, A.G. and Charles, E.A., J. Am. Cer Soc., 59 (1976) 371.
36. Mathia, T.G., and Lamy, B., Wear, 108 (1986) 385.
37. Ridgway, K., and Tarbuckle, K.J., Brit. Chem. Eng., 12 (1967) 384.

38. Arzt, E., Acta Metall., 30 (1982) 1883.
39. Voronoi, G.F., J. Reine Angew. Math., 134 (1908) 198.
40. Scott, G.D., Nature, 188 (1960) 908.
41. Schwartz, E.G., and Holland, A.R., Int. J. Powder Metall., 5 (1969) 79.
42. Hardman, J. S., and Lilley, B.A., in Proc. 1st Intl. Conf. on the Compaction and Consolidation of Particulate Matter, Brighton, 3-5 Oct., 1972, Powder Technol. Publ. Series, #4, A.S. Goldberg, ed., 1972, 115.
43. Green, A.P., J. Mech. Phys. Solids, 2 (1954) 197.
44. Rudnick, A., Marshall, C.W., Duckworth, W.H., and Emrich, B.R., " The evaluation and interpretation of the mechanical properties of brittle materials", Defense ceramic information center report DCIC 68-3, 1968
45. Griffith, A.A., The theory of rupture, Proc. of the 1st Intl. Congress on Applied Mechanics, C.B. Biezeno, J.M. Burgers, eds., J. Waltman, Delft, (1927) 55.
46. Rice, R.W., in Materials Science Research, Vol. 5, Ceramics in Severe Environments, Krigel, W.W., and Palmour, H., eds., Plenum Press, N.Y., 1971, 197 .
47. Venkatachari, K.R., and Raj, R., J. Am. Cer. Soc., 69 (1986) 499.
48. Obiorah, B.A., Int.J.Pharm., 1 (1978) 24.
49. Leigh, S., Carless, J.E., and Burt, B.W., J. Pharm. Sci, 56 (1967) 888.
50. Summers, M.P., Enever, R.P., and Carless, J.E., J. Pharm. Pharmacol., 28 (1976) 89.
51. Ridgway, K., and Rupp, R., J.Pharm. Pharmacol., 21 (1969) 30S.
52. Cole E.T., Rees, J.E., Hersey, J.A., Pharm. Acta Helv., 1975, 50, 28.
53. Papadimitropoulos , E.M., and Duncan-Hewitt, W.C., J. Pharm. Sci, *in press*.

54. Frost, H.J., and Ashby, M.F., Deformation Mechanism Maps, Pergamon Press, Oxford, 1982.
55. Johnson W.G., and Gilman, J.J., J. App. Phys., 1959, 30, 129.